

Title:

Gradient magnetic field measurement using first-order gradiometers equipped with 50 mm diameter pickup coils made out of a 2G High- T_c Superconducting Tape

Kazunori Komori^{a*}, Shunichi Arisawa^a, Minoru Tachiki^a, Shuuichi Ooi^a, Tadayuki Hayashi^b and Kazuhiro Endo^c

^a National Institute for Materials Science, Tsukuba, Ibaraki, Japan

^b National Institute of Technology, Sendai College, Sendai, Miyagi, Japan

^c Kanazawa Institute of Technology, Nonoichi, Ishikawa, Japan

Corresponding to: *E-mail: KOMORI.Kazunori@nims.go.jp

Abstract

Two types of first-order gradiometers equipped with 50 mm diameter pickup coils were made out of an REBaCuO High- T_c superconducting (HTS) flexible tape. The HTS tapes were formed into the HTS gradiometers by "cut-and-wind" method without cable jointing. The HTS gradiometers were examined at 77 K for magnetic sensitivity to a gradient field applied by an external coil. The axial-type HTS gradiometer eliminated the magnetic field output of the device induced by a uniform field, and enhanced the magnetic field output induced by a gradient field on the axis of the pickup coil. The planar-type HTS gradiometer made it possible to detect a 20 mm diameter steel cylinder placed beside the pickup coil in a uniform field of 100 μ T by detecting the spatial field gradient in the vicinity of a ferromagnetic object.

Keywords: superconducting gradiometer, magnetic flux transformer, High- T_c superconducting tape, static field measurement

1. Introduction

Magnetic diagnostics using static or extremely low frequency magnetic fields are expected to be used for non-destructive evaluation of structural materials and food contamination in terms of magnetic field permeability in objects. Magnetic signals can penetrate a material with low magnetic permeability with low attenuation. Therefore, magnetic signals can be used to obtain information about magnetic substances which is deep inside non-magnetic objects, such as rebar in concrete [1] or broken metal needles in food [2]. For the conductive objects such as metals, the penetration of the magnetic signal inside the object is limited to the skin depth: the penetration depth of the magnetic field caused by signal attenuation at the conductor surface due to electromagnetic induction. Since the skin depth increases with decreasing frequency of the applied magnetic field, magnetic inspection using low frequency magnetic fields can provide information about the deep region of the conductors. In non-destructive evaluation and mining resource exploration, several attempts have been made to obtain information about the deeper region by using highly sensitive static magnetic field sensors, such as the Superconducting Quantum Interfering Device (SQUID), to replace conventional inductive detection coils that are sensitive to high-frequency electromagnetic fields [3-4]. However, such highly sensitive magneto-sensors can be disturbed by ambient magnetic noise or affected by bias signal contamination due to geomagnetism. For the magnetic noise contamination, the SQUID instrument uses a design in which the sample and the sensor are placed in magnetic shields and the magnetic signal to be measured is transmitted using a superconducting flux transformer to improve the magnetic disturbance [5-6]. A superconducting flux transformer transfers magnetic flux between two coils, the pickup coil and the input coil, in a closed superconducting circuit. Compared to magnetic signal transmission using flux guides made of highly permeable materials or electromagnetic induction coils, the superconducting flux transformer provides highly efficient magnetic signal transmission ranging from relatively low frequency fields to a static field [7]. The superconducting flux transformer collects the magnetic flux to be measured, transmits it while suppressing ambient noise, and amplifies the magnetic field by flux condensation, thus enabling highly sensitive magnetic measurements.

On the other hand, to overcome the problems of signal distortion due to geomagnetism, the differential measurement using two magneto-sensors [8] has been proposed for magnetic measurements that can be used outside a magnetically shielded room, where the effect of geomagnetism is of concern. In this method, one sensor is used to measure the

magnetic field of the object and the other sensor is used to measure the background magnetic field around the object, and the calibrated values are obtained by signal calculation. A calibrated signal is zero when the measured magnetic fields of the two sensors are equal, and a signal is generated only when the signal between the sensors is different, thus eliminating the signal bias component due to the ambient uniform magnetic field. Although this method is effective in eliminating the bias signal contamination caused by the ambient magnetic field, the use of multiple sensors can cause problems such as adjustment for individual differences in the sensors and changes in the balance between the sensors due to drift in the characteristic of each sensor.

In contrast, a superconducting gradiometer which is based on the superconducting flux transformer has been proposed [9]. In the design of the superconducting gradiometer, multiple pickup coils are geometrically arranged to cancel the self-induced superconducting shield currents caused by the application of a uniform magnetic field to the coils. A superconducting gradiometer functions as a signal calibrator for the ambient magnetic field so that a superconducting gradiometer system requires only one magnetosensor without concern for the balance between the sensors. Conventional superconducting flux transformers and superconducting gradiometers have been made of metallic superconducting wires such as niobium [10-11]. Since metallic superconducting wires have a low critical temperature (T_c) of the superconducting transition, the conventional superconducting gradiometers require cooling to liquid helium temperature for operation. In contrast, High- T_c superconducting (HTS) materials have a critical temperature higher than liquid nitrogen temperature [12-13]. Liquid nitrogen cooling is simple and convenient compared to liquid helium cooling in terms of thermal insulation design. In addition, an HTS device can also be operated with a small, low-vibration refrigerator, which improves the portability of the measuring instrument and makes it more convenient for on-site measurements. For these reasons, an HTS gradiometer is expected to have applications in highly sensitive magnetic evaluation, usable outside of magnetically shielded rooms for deep magnetic contamination and defects.

The preparation of a superconducting closed circuit is essential for a superconducting gradiometer. One straightforward approach to this process is to make a superconducting joint between the ends of bent wires. However, a convenient joining method for the HTS wires has not been fully established. Methods such as pressure welding and soldering using Bi-Pb superconducting alloys [14], which are effective for making superconducting joints with metallic superconducting wires, cannot be applied to the HTS wires. Previous reports on HTS wire joints [15-17] have limitations in terms of the fabrication of superconducting closed circuits, including the degradation of superconducting properties

at the joints, significant change in joint size, and the process time. For these reasons, the HTS gradiometers reported in previous studies, which operate at liquid nitrogen temperatures, use thin films fabricated on oxide single crystals or flexible metal tapes, and closed circuits are patterned by etching [18-19]. These fabrication methods enable the preparation of closed circuits that become fully superconducting at liquid nitrogen temperatures because there are no joints, but it is difficult to prepare large devices because the coil diameter is limited by the width of the substrate. Furthermore, the fabrication of the multi-turn coil required for signal amplification in the superconducting gradiometer requires implementation of additional complex processes for the construction of wiring bridges and insulating layers [20].

In light of these constraints, an improvement to the HTS gradiometer utilizing flux guides has been proposed [21]. The focusing of the magnetic flux by the flux guide increases the inductance of the coil and is anticipated to have a comparable effect to equipping a large coil. However, there is a concern that the residual magnetization of the flux guide may influence the measurement of small magnetic fields. Consequently, the integration of large-bore air-core pickup coil in a HTS gradiometer is advantageous for magnetic measurements on large objects, such as geomagnetic surveys, due to its efficacy in enhancing sensitivity by harvesting magnetic flux in weak magnetic fields, circumventing the issue of residual magnetization.

Previous studies have reported the fabrications of a seamless superconducting loop by this method, which involves geometrically bending a commercially available HTS monofilament tape with a slit [22-23]. To date, we have fabricated HTS flux transformers equipped with a large-bore coil and a multi-turn coil by a technique, which we call the "cut-and-wind" method and reported the magnetic field transfer of the HTS flux transformer in static fields [24]. In this study, we have prepared two types of the HTS gradiometer by modifying the fabrication method and estimated their magnetic properties. The gradiometer comprises two pickup coils in a closed circuit, with the geometry of the coils designed to ensure that the superconducting shield currents induced in each pickup coil cancel out in a uniform field. There are two types of the device in terms of configuration of the pickup coils. The axial-type HTS gradiometer has been examined in terms of gradient field measurement, with the aim of eliminating bias signal caused by ambient uniform field. The uniform and the gradient field have been applied by each of the external coils.

The planar-type HTS gradiometer has been examined to detect a steel cylinder placed in proximity to the pickup coil in a uniform magnetic field. It has been demonstrated that a spatial gradient magnetic field exists in the vicinity of a ferromagnetic body in a uniform

field. The planar-type HTS gradiometer has been estimated as a detector of a magnetic sample through the field gradient depending on the sample placement relative to the pickup coil.

2. Experimental details

2.1 Fabrication of the HTS gradiometers

Two types of the HTS gradiometer were prepared: an axial-type HTS gradiometer and a planar-type HTS gradiometer. Figures 1 and 2 show the fabrication of the HTS gradiometers by the "cut-and-wind" method employed in this study. The commercially available $\text{REBa}_2\text{Cu}_3\text{O}_y$ (REBCO) 2G-HTS mono-filamentary tape (*SuperPower Inc.*) with a width of 12 mm was utilized for the fabrication of the HTS gradiometers.

Figure 1 shows the fabrication method of the axial-type HTS gradiometer, in which two pickup coils are aligned axially so that their central axes coincide. Three through-hole slits were made on one end of the tape, and a hole pattern acting as an input coil was created on the other end. Additionally, narrow trenches were patterned as shown in Figure 1 to connect the slits and the hole. The slits were cut with a 0.1 mm thick diamond wheel. The hole pattern and narrow trenches were created by chemical etching from the surface to the superconducting layer of the tape. The tape comprises a Hastelloy C-276 substrate (50 μm thick) with a textured buffer layer, a REBCO superconducting layer (0.5 μm thick), a silver protective layer (2 μm thick), and an outer copper layer (20 μm thick). The copper, silver, and superconducting layers were removed using a mixture of 5% hydrochloric acid and 35% hydrogen peroxide solution, 1% ammonia solution and 35% hydrogen peroxide solution, and 1% hydrochloric acid, respectively. It should be noted that the patterned HTS line on the tape forms a closed circuit. Subsequently, the four lines divided by the slits were bent in a direction perpendicular to the tape surface, as shown in Figure 1. Thereafter, hollow cylinders of glass epoxy were inserted into the lines and fixed.

Two loop sections, comprising the first and second lines and the third and fourth lines, respectively, were wound in opposite directions to one another. This configuration enabled the pickup coils region to function as a differential probe for field distribution. Additionally, an HTS flux transformer with a 2-turn pickup coil was prepared by changing the loop configuration to have the same winding direction of both loops. The HTS gradiometer and the flux transformer were fabricated in the same size to enable a comparison of their respective responses to uniform and gradient static magnetic fields. The diameters of their pickup and input coils were 50 mm and 5 mm, respectively.

Figure 2 shows the fabrication of a planar-type HTS gradiometer, in which two pickup coils were adjacent and arranged horizontally. A long through-hole slit and a hole pattern were created in opposite ends of a 12 mm wide 2G-HTS tape, with a narrow trench connecting the slit and the hole pattern in a manner analogous to the fabrication of the

axial-type HTS gradiometer. The fabrication method of the slit, hole pattern and narrow trench is analogous to that of the axial-type HTS gradiometer. The two wires separated by the slit were bent into an S-shape in the direction shown in Figure 2. Two glass epoxy hollow cylinders were then inserted and fixed to the wires, thereby forming two adjacent pickup coils with opposite winding directions. The diameters of the pickup and input coils were 52 mm and 5 mm, respectively.

2.2 Measurement of a magnetic field output of an axial-type HTS gradiometer generated by static field applying

A magnetic field output of the axial-type HTS gradiometer was measured for both gradient and uniform field by the external coils. Figure 3 shows an overview of the measurement setup. The experimental apparatus was installed in a magnetically shielded room. A Helmholtz coil applying a uniformly distributed magnetic field consisted of two coils of 308 mm diameter connected in the same winding direction at a distance of 154 mm. Conversely, the same 308 mm diameter coils were connected in the opposite winding direction with a spacing of 266.7 mm to form a Maxwell pair coil applying a gradient magnetic field.

The axial-type HTS gradiometer was installed in each coil so that the center and axial direction of its pickup coils and the field-applying coil were coincident. The entire HTS gradiometer was cooled with liquid nitrogen, and then a static magnetic field was applied to the pickup coils. This operation induced a superconducting shield current in the HTS gradiometer, which depended on the applied field. The magnetic field generated in the input coil by the superconducting current was measured using a magneto-impedance (MI) sensor (MGM-1DS, *Aichi Micro Intelligent Corp.*), which was placed opposite the input coil with a thermal insulating polystyrene foam (5 mm thick) between them. The magnetic field of the input coil was measured for the application of uniform and gradient magnetic fields, respectively. For purposes of comparison, the magnetic field in the input coil was also measured on the HTS flux transformer with a 2-turn pickup coil. This coil was of the same size and wound in a different direction to the pickup coils of the gradiometer, as shown in Figure 1.

2.3 Detection of a steel piece in a uniform magnetic field using a planar-type HTS gradiometer

The detection of a steel piece was attempted using a planar-type HTS gradiometer by detecting the spatial field gradient in the vicinity of a ferromagnetic object in a uniform magnetic field. Figure 4 shows the schematic of the experimental apparatus, which was placed inside a magnetic shield. A planar-type HTS gradiometer was installed in the Helmholtz coil with a diameter of 308 mm, ensuring that the center of the Helmholtz coil coincided with the center points of the two pickup coils of the gradiometer. The entire gradiometer was cooled with liquid nitrogen and a 2 mm thick acrylic plate was placed over it. An S45C steel cylinder (20 mm in diameter and 10 mm in height) was placed on the acrylic plate. The distance from the center of the height of the gradiometer to the bottom of the steel cylinder was 32 mm across the acrylic plate. A uniform magnetic field was applied to the pickup coils by a Helmholtz coil, and the magnetic field output of the gradiometer was measured using a MI sensor with the position of the steel cylinder above the pickup coil varied. As shown in Figure 5, the position of the steel cylinder was altered along two distinct lines: a gradiometer center line traversing the center of each pickup coil (Figure 5 (a)), and a line extending from the center of the pickup coil at the end and perpendicular to the gradiometer center line (Figure 5 (b)).

3. Results and Discussion

3.1 Magnetic field outputs of an axial-type HTS gradiometer in both gradient and uniform static fields

A magnetic field generated in the input coil of an axial-type HTS gradiometer has been measured in both the uniform and gradient fields. Figure 6 shows the outcome of the measurements of both the HTS gradiometer and the HTS flux transformer in a uniform static magnetic field applied by a Helmholtz coil. The HTS flux transformer is equipped with a 2-turn pickup coil of the same diameter as that of the HTS gradiometer. In both devices, the direction of the generated field in the input coil is perpendicular to the applied field. Additionally, the input coil of each device is separated from the field-applying coil, thereby reducing the contamination of the measured field by the applied field.

In the HTS flux transformer equipped with a 2-turn pickup coil, the directions of a superconducting current induced by applying a uniform field are identical in each turn of the pickup coil. The induced superconducting current is proportional to the applied field, and the magnetic field of the input coil generated by the current is also proportional to the applied field, as shown Figure 6. In contrast, the first-order axial-type HTS gradiometer prepared in this study has two pickup coils of equal inductance and connects them in opposite directions. The design of a first-order superconducting gradiometer, comprising two pickup coils of equal inductance connected in opposite directions, ensures that the induced current in each coil has equal magnitude and opposite direction to the corresponding pickup coil when a uniform field is applied. Consequently, the current in each coil cancels each other out, resulting in a zero magnetic field generated in the input coil. As shown in Figure 6, when a uniform static field is applied, the magnetic field in the input coil of the axial-type HTS gradiometer is close to zero. This implies that the superconducting currents of each pickup coil are nearly identical, and that the current induction in each coil is symmetrical to the applied field, despite the asymmetric shape of the pickup coils in the design of the HTS gradiometer.

Conversely, Figure 7 shows the measurement of the magnetic field generated in the input coil of both the HTS gradiometer and the HTS flux transformer in a gradient magnetic field applied to the pickup coil using a Maxwell pair coil. In contrast to the results presented in Figure 6, the magnetic field in the input coil of the gradiometer was considerably larger than that of the HTS flux transformer, despite the fact that the HTS flux transformer also generated a magnetic field in the input coil. The magnetic field is distinct in the upper and lower pickup coils of the gradiometer in a gradient field. Since

the pickup coils are connected in opposite directions, the magnetic flux penetrating the closed loop of the entire gradiometer is depending on the difference of each of the fluxes in the coil. The magnetic flux that penetrates the entire loop generates a superconducting current that forms a magnetic field in the input coil, thereby enabling the gradiometer to produce a large magnetic field signal in a gradient magnetic field. In contrast, the magnetic field in the input coil of the HTS flux transformer with a 2-turn pickup coil is smaller than that of the gradiometer. The magnetic flux through the closed loop of the entire HTS flux transformer will be the sum of the magnetic flux through each loop of the pickup coil. In the gradient field, the induced current and the magnetic flux must be equal in the upper and lower loops of the pickup coil, despite the differing the magnetic fields in the upper and lower loops. Consequently, the magnetic flux through the entire pickup coil of the HTS flux transformer in the gradient field and the induced superconducting current will be reduced in proportion to the difference of flux between each loop. Therefore, the magnetic field generated by the superconducting current to the HTS flux transformer in a gradient magnetic field is smaller than that in a uniform magnetic field. In this study, the magnetic field was applied to the pickup coil at the center of the Maxwell pair coil, resulting in an opposing magnetic field at the upper and lower loops of the pickup coil. This phenomenon can be considered a contributing factor to the observed reduction in the magnetic field of the HTS flux transformer in a gradient field.

The results in Figures 6 and 7 show that the HTS gradiometer produces a larger magnetic field signal than the HTS flux transformer as the gradient of the magnetic field increases. The HTS gradiometer fabricated in this study generates the magnetic field signal solely by the difference in field intensity in each of the pickup coils, without a common bias component of the field between them. Consequently, the axial-type HTS gradiometer is capable of detecting only the static magnetic field gradient along the axis of the pickup coil, thereby eliminating the contamination of the bias component and the average intensity of the ambient field from the measured value in unshielded magnetic measurements. This feature of the HTS gradiometer is anticipated to be employed in magnetic evaluation techniques conducted in static magnetic fields, including deep non-destructive inspection of structures and food products, and geomagnetic measurements for resource exploration.

3.2 Detection of ferromagnetic object in a uniform field using a planar-type HTS gradiometer

In the vicinity of a ferromagnetic material in a uniform magnetic field, a spatial magnetic

field gradient is generated due to its magnetic permeability. We considered that detection of magnetic objects was possible with measuring the magnetic field gradient by an HTS gradiometer and attempted to detect a magnetic object in a uniform field using a planar-type HTS gradiometer. As shown in Figure 4, a steel cylinder was positioned above the pickup coil of the planar-type HTS gradiometer in a uniform static magnetic field generated by the Helmholtz coil. The pickup coil at one end of the gradiometer was employed as a probe to detect the magnetic field in the vicinity of the magnetic object, while the other pickup coil served used as a reference coil to measure the background field around the device. The magnetic field generated in the input coil due to the difference in field intensity between the two pickup coils was measured as the steel cylinder was moved in different positions, as shown in Figure 5.

Figures 8 and 9 show the magnetic field of the input coil in relation to the position of the steel cylinder relative to the HTS gradiometer in a uniform magnetic field. Figure 8 shows the results of varying the position of a cylinder as shown in Figure 5(a) along the center line of the gradiometer from outside the end pickup coil, through the center and into the other pickup coil. The horizontal axis of the Figure 8 represents the relative position of the center of the cylinder to the center of the pickup coil as a probe. When the cylinder was positioned outside the outer edge of the probe, the magnetic field of the input coil exhibited a nearly zero value or a slight negative value. As the cylinder approached the center of the probe, the magnetic field increased, reached a maximum at the center of the probe, and then decreased. Moreover, the magnetic field became zero when the cylinder was at the boundary of the pickup coils, and a negative value when the cylinder entered the region of the reference coil. This variation in the field signal is attributed to a spatial field gradient resulting from the focussing of magnetic flux from the applied field into the ferromagnetic object. When the ferromagnetic object was situated at a considerable distance from the probe, the magnetic field gradient near the object was sufficiently reduced at the distance to the probe, such that the magnetic field gradient near the probe was minimal. Consequently, the magnetic field generated in the input coil of the gradiometer was also minimal. As the cylinder approached the center of the probe, the magnetic flux focused into the object and transmitted to the probe increased, and the magnetic field gradient between the probe and reference coil also increased. At the midpoint between the probe and the reference coil, the magnetic field gradient was zero because the focused flux is equally distributed to both coils. When the cylinder was positioned above of the reference coil, the concentrated flux was predominantly directed towards to the reference coil, resulting in a reversal of the magnetic field gradient between the probe and reference coil. Furthermore, an increase in the applied magnetic field from

100 μT to 200 μT resulted in a nearly twofold increase in the magnetic field signals in the input coil at each position of the cylinder, accompanied by a proportional increase in the ratio of the magnetic field change to the distance traversed by the cylinder. This indicates that an increase in the applied magnetic field is an effective method for detecting a magnetic object using the HTS gradiometer.

Figure 9 shows the outcomes of varying the position of the steel cylinder on the probe in the direction depicted in Figure 5(b), extending from the exterior of the probe through the center and exiting the opposite side. When the cylinder was positioned outside and adjacent to the edge of the probe, the field within the input coil exhibited a negative value. Although not shown in Figures 8 and 9, the magnetic field of the input coil in the absence of the steel cylinder was nearly zero (with a magnitude of $<0.1\mu\text{T}$). Consequently, when the cylinder approaches the probe from a distance, the magnetic field of the input coil transitions to a positive value after initially changing to a negative value. This variation in the field signal can also be attributed to the magnetic flux focusing into the cylinder and a reduction in magnetic flux density in the surrounding space. In contrast to the results in Figure 8, the change in the magnetic field became less pronounced when the entire cylinder was within the probe area. Additionally, the ratio of the change in the magnetic field to the distance the cylinder moved across the probe edge increased. This discrepancy in the signal between the two movement directions is believed to be attributed to the shape of the pickup coil. When the cylinder is in motion along the center line of the gradiometer, the overlap between the cylinder and the probe area undergoes a gradual change at the tip of the probe due to the shape of the pickup coil, as shown in Figure 2. In contrast, the overlap between the cylinder in motion perpendicular to the center line and the probe area undergoes a pronounced change above the arc of the probe edge. Furthermore, the distance between the cylinder and the reference coil undergoes a significant change when the cylinder is in motion along the center line. This alteration in the distance is likely to influence the field on the reference coil and the measurement of the magnetic field gradient.

The shape of the pickup coil of the gradiometer utilized in this study is asymmetric in both directions, with respect to the center line of the gradiometer and a line perpendicular to the center line. However, the magnetic field outputs of the gradiometer for the positions of the cylinders shown in Figures 8 and 9 were symmetrical with respect to the center of the pickup coil and the center of the probe, respectively. This discrepancy can be attributed to the fact that the superconducting shielding current concentrates at the narrow cross-sectional area in the interface between the superconductor and the magnetic field penetrating the space inside the coil. Since the superconducting current is concentrated

near the slit on the HTS tape and the cross-sectional area of the current flow is very narrow compared to the width of the conducting tape, the current path can be considered to become almost planar. It has been demonstrated that the position symmetry of the magnetic field output in the planar-type HTS gradiometer is due to the planar current path in the pickup coils.

Furthermore, it has been shown that the planar-type HTS gradiometer is capable of detecting magnetic objects with large magnetic signal transitions in the vicinity of the edge of the probe coil. These results indicate that scanning the HTS gradiometer in multiple directions may facilitate the detection of magnetic objects, such as deep magnetic contamination and structural defects, through magnetic inspection.

4. Conclusion

Two types of first-order HTS gradiometers (axial- and planar-type) were fabricated using commercially available 2G-HTS tape. The cut-and-wind method allows the entire gradiometer to remain superconducting at 77 K because there are no junctions in the closed circuit. It is also possible to construct a high-order device design, such as a second-order HTS gradiometer equipped with multiple geometrically connected pickup coils. The magnetic field signal generation of the axial-type HTS gradiometer was investigated at liquid nitrogen temperature in a uniform magnetic field and in a gradient magnetic field. The magnetic field generation on the input coil was found to be significantly suppressed when a uniform magnetic field was applied, while a large magnetic field signal was observed when an axial gradient magnetic field was applied. Furthermore, the detection of a ferromagnetic steel cylinder placed in a uniform magnetic field was examined using a planar type HTS gradiometer. In the vicinity of the pickup coil on one side, which was used as a probe, the magnetic field signal output of the gradiometer exhibited a significant change in dependence on the position of the magnetic object.

In addition to the simplicity of the cooling system, the elimination of bias components due to uniform static magnetic fields such as geomagnetism represents a unique feature of HTS gradiometers in application. The HTS gradiometer proposed in this study allows for the fabrication of high-order HTS gradiometers and devices with a large pickup coils, up to several meters in diameter. These characteristics make the HTS gradiometer a promising candidate for in-situ magnetic measurements such as non-destructive testing and resource exploration, which do not require a magnetic shield surrounding a large object.

Acknowledgements

We are thankful to Prof. Gen Uehara and Prof. Yoshiaki Adachi from the Kanazawa Institute of Technology for their helpful discussions during this study.

References

- [1] D. He, M. Shiwa, S. Takaya, and K. Tsuchiya, *Studies in Applied Electromagnetics and Mechanics*, 42: Electromagnetic Nondestructive Evaluation (XX) (2017), pp. 247-252. <https://doi.org/10.3233/978-1-61499-767-2-247>.
- [2] M. Graves, A. Smith, and B. Batchelor, *Trends Food Sci. Technol.* 9 (1998) pp. 21-27. [https://doi.org/10.1016/S0924-2244\(97\)00003-4](https://doi.org/10.1016/S0924-2244(97)00003-4).
- [3] M. Hayashi, T. Saito, Y. Nakamura, K. Sakai, T. Kiwa, I. Tanikura, and K. Tsukada, *Sensors* 19 (2019) 3001. <https://doi.org/10.3390/s19133001>.
- [4] T. Hato, A. Tsukamoto, S. Adachi, Y. Oshikubo, H. Watanabe, H. Ishikawa, M. Sugisaki, E. Arai, and K. Tanabe, *Supercond. Sci. Technol.* 26 (2013), 115003. <https://doi.org/10.1088/0953-2048/26/11/115003>.
- [5] R. Kleiner, D. Koelle, F. Ludwig, and J. Clarke, *Proceedings of the IEEE* 92 (2004), pp. 1534-1548. <https://doi.org/10.1109/JPROC.2004.833655>.
- [6] D. Drung, *IEEE/CSC & ESAS SUPERCONDUCTIVITY NEWS FORUM (SNF)* 36 (2016), CR70.
- [7] J.E. Zimmerman, *Cryogenics* 20 (1980), pp. 3-10. [https://doi.org/10.1016/0011-2275\(80\)90062-4](https://doi.org/10.1016/0011-2275(80)90062-4).
- [8] T. Takiya, T. Uchiyama, and H. Aoyama, *J. Magn. Soc. Jpn.* 40 (2016), pp. 51-55. <https://doi.org/10.3379/msjmag.1605R001>.
- [9] J.E. Zimmerman, *J. Appl. Phys.* 48 (1977), 702. <https://doi.org/10.1063/1.323659>.
- [10] D. Chen, G. Jia, X.K. Liu, L. Chen, and X.D. Liu, *Supercond. Sci. Technol.* 33 (2020), 085011. <https://doi.org/10.1088/1361-6668/ab9e42>.
- [11] G. Zhang, Y. Zhang, S. Zhang, H.J. Krause, Y. Wang, C. Liu, J. Zeng, Y. Qiu, X. Kong, H. Dong, X. Xie, A. Offenhäusser, and M. Jiang, *Physica C* 480 (2012) pp. 10-13. <https://doi.org/10.1016/j.physc.2012.04.023>.
- [12] M.K. Wu, J.R. Ashburn, C.J. Torng, P.H. Hor, R.L. Meng, L. Gao, Z.J. Huang, Y.Q. Wang, and C.W. Chu, *Phys. Rev. Lett.* 58 (1987) 908. <https://doi.org/10.1103/PhysRevLett.58.908>.
- [13] H. Maeda, Y. Tanaka, M. Fukutomi, and T. Asano, *Jpn. J. Appl. Phys.* 27 (1988), L209. <https://doi.org/10.1143/JJAP.27.L209>.
- [14] G.D. Brittles, T. Mousavi, C.R.M. Grovenor, C. Aksoy and S.C. Speller, *Supercond. Sci. Technol.* 28 (2015), 093001. <https://doi.org/10.1088/0953-2048/28/9/093001>.
- [15] J.Y. Kato, N. Sakai, S. Tajima, S. Miyata, M. Konishi, Y. Yamada, N. Chikumoto, K. Nakao, T. Izumi, and Y. Shiohara, *Physica C* 445-448 (2006), 686-688.

<https://doi.org/10.1016/j.physc.2006.05.005>.

- [16] X. Jin, Y. Yanagisawa, H. Maeda, and Y. Takano, *Supercond. Sci. Technol* 28 (2015), 075010. <https://doi.org/10.1088/0953-2048/28/7/075010>.
- [17] Y.J. Park, M.W. Lee, Y.K. Oh, and H.G. Lee, *Supercond. Sci. Technol.* 27 (2014), 085008. <https://doi.org/10.1088/0953-2048/27/8/085008>.
- [18] A. Kittel, K.A. Kouznetsov, R. McDermott, B. Oh, and J. Clarke, *Appl. Phys. Lett.* 73 (1998), 2197. <https://doi.org/10.1063/1.122421>.
- [19] M. Bick, K.E. Leslie, R.A. Binks, D.L. Tilbrook, S.K.H. Lam, R. Gnanarajan, J. Du, and C.P. Foley, *Appl. Phys. Lett.* 84 (2004), 5347. <https://doi.org/10.1063/1.1766401>.
- [20] M. Teraoka, A. Tsukamoto, S. Adachi, H. Takai, K. Tanabe, "26th International Symposium on Superconductivity, ISS 2013", *Physics Procedia* 58 (2014), 204-207. <https://doi.org/10.1016/j.phpro.2014.09.056>.
- [21] S.I. Bondarenko, A.A. Shablo, P.P. Pavlov, and S.S. Perepelkin, *Physica C* 372–376 (2002), 158-161. [https://doi.org/10.1016/S0921-4534\(02\)00643-3](https://doi.org/10.1016/S0921-4534(02)00643-3).
- [22] H.G. Lee, J.G. Kim, S.W. Lee, W.S. Kim, S.W. Lee, K.D. Choi, G.W. Hong, and T.K. Ko, *Physica C* 445–448 (2006), 1099-1102. <https://doi.org/10.1016/j.physc.2006.05.044>.
- [23] C.C. Rong, P.N. Barnes, G.A. Levin, J.D. Miller D.J. Santosusso, and B.K. Fitzpatrick, *IEEE Trans. on Appl. Supercond.*, 25 (2015), 8200805. <https://doi.org/10.1109/TASC.2014.2376173>.
- [24] K. Komori¹, S. Arisawa, M. Tachiki, S. Ooi, T. Hayashi, and K. Endo, *Jpn. J. Appl. Phys.* 60 (2021), 073002. <https://doi.org/10.35848/1347-4065/ac0406>.

Figure captions.

Figure 1

Fabrication of an axial-type HTS gradiometer and an HTS flux transformer with multi-turn pickup coil by “cut-and-wind” method using 2G-HTS tape. Hollow spacers for coil fixation are not shown in the figure.

Figure 2

Fabrication of a planar-type HTS gradiometer by “cut-and-wind” method using 2G-HTS tape. Hollow spacers for coil fixation are not shown in the figure.

Figure 3

Overview of the setup to measure the magnetic field in the input coils of an axial-type HTS gradiometer and an HTS flux transformer. A Helmholtz coil and a Maxwell pair coil were used to apply the uniform static field and the gradient static field application, respectively. The magnetic field generated in the input coil was measured by MI sensor which was coupled to the coil.

Figure 4

Overview of the setup to detect a steel cylinder using a planar-type HTS gradiometer. Local gradient of magnetic field generated in the vicinity of a ferromagnetic object in uniform field was measured by the HTS gradiometer. Variation of the magnetic field in the input coil depending on the relative position of steel cylinder to the probe coil(the pickup coil in end) was also measured.

Figure 5

Top view of each position of the steel cylinder in measuring. The position of the steel cylinder was changed along two lines: a gradiometer center line through each center of the pickup coil (a), and a line through the center of the pickup coil at the end and perpendicular to the gradiometer center line (b).

Figure 6

Magnetic field in the input coil caused by a uniform magnetic field application for the axial-type HTS gradiometer and the HTS flux transformer. In the HTS flux transformer, the magnetic field in the coil increased proportionally to the applied field. In contrast, the value of the magnetic field in the coil and its variation with respect to the applied field

were much smaller in the HTS gradiometer.

Figure 7

Magnetic field in the input coil caused by a gradient magnetic field application for the axial-type HTS gradiometer and the HTS flux transformer. The magnetic field in the coil increased proportionally to the applied field in the HTS flux transformer, however, the rate of the increase was much larger in the HTS gradiometer.

Figure 8

Variation of the magnetic field in the input coil of the planar-type HTS gradiometer depending on the position of the steel cylinder. This figure shows the field variation when the steel cylinder is moved along the centerline of the gradiometer.

Figure 9

Variation of the magnetic field in the input coil of the planar-type HTS gradiometer depending on the position of the steel cylinder. This figure shows the field variation when the steel cylinder is moved in the direction perpendicular to the centerline of the gradiometer.

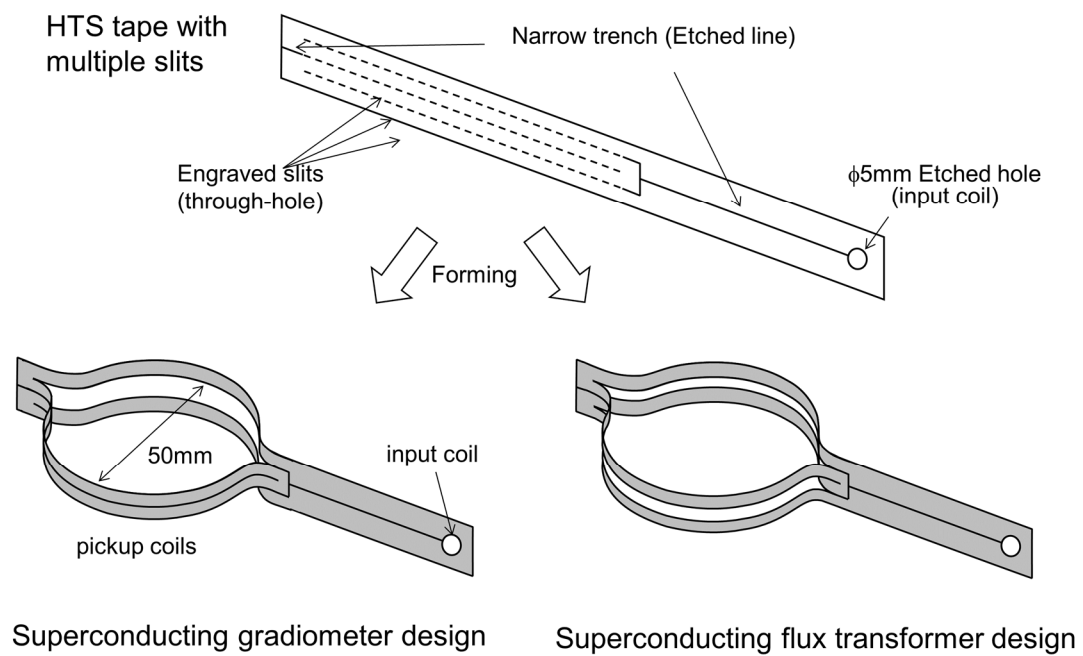


Fig.1

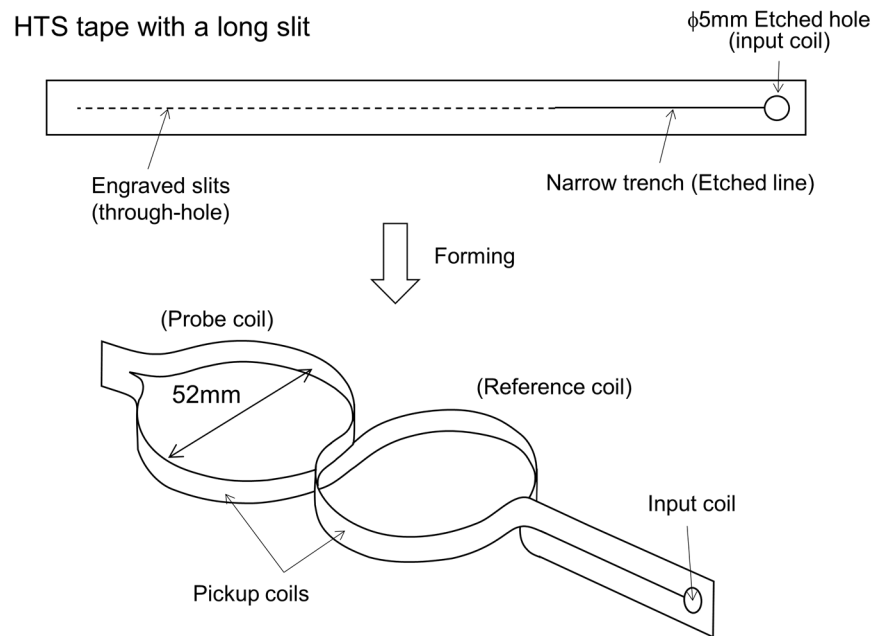


Fig. 2

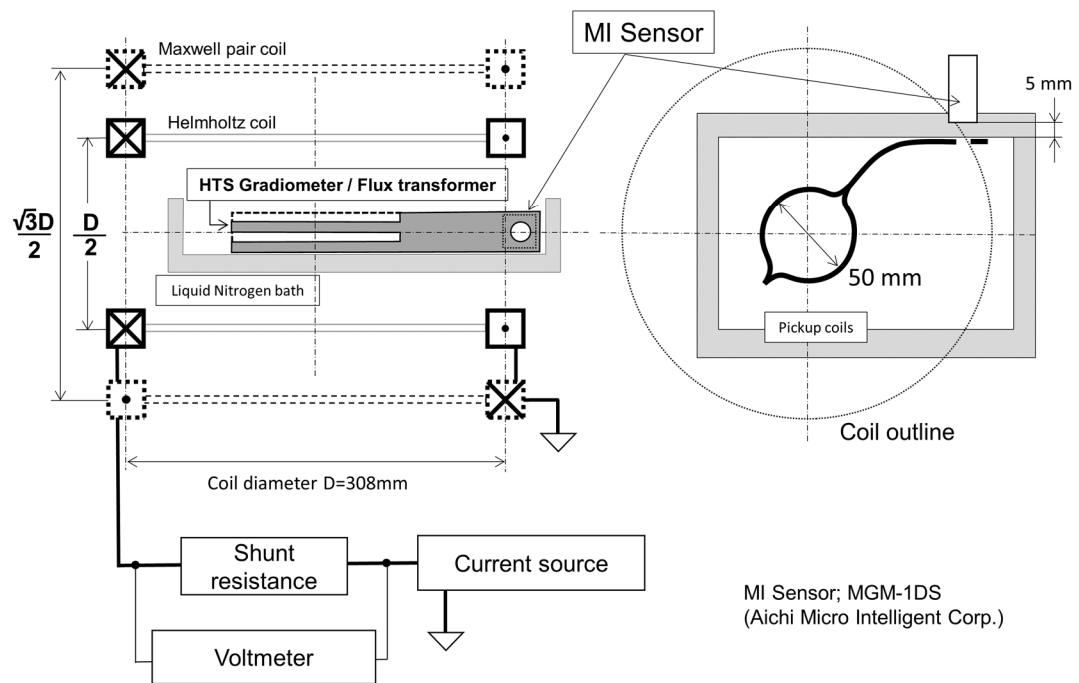


Fig. 3

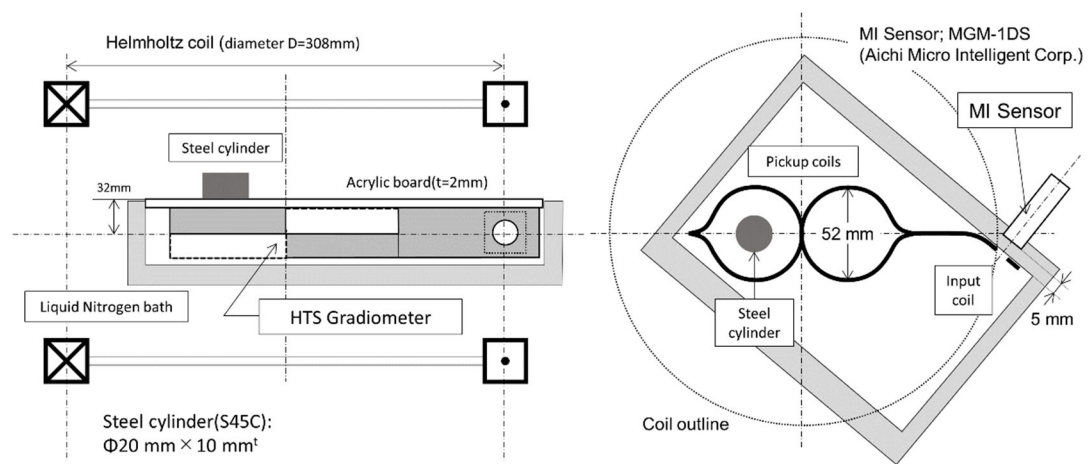


Fig. 4

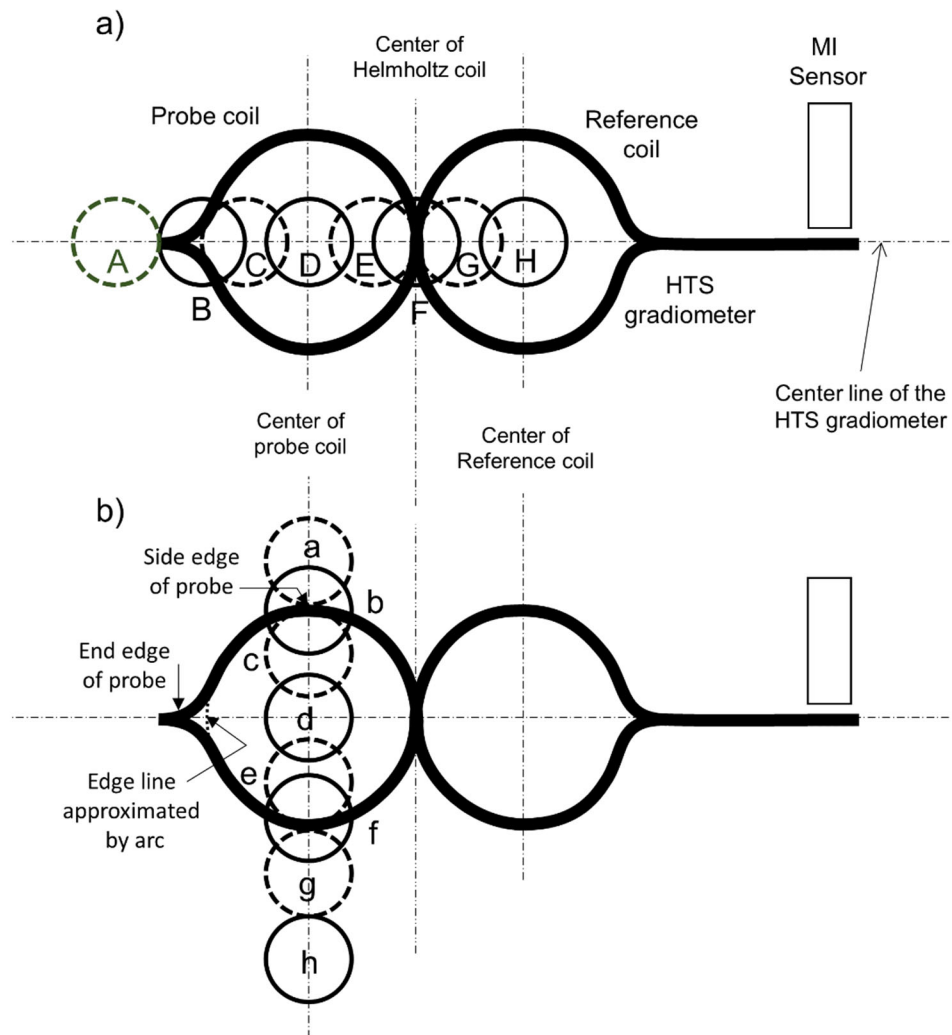


Fig. 5

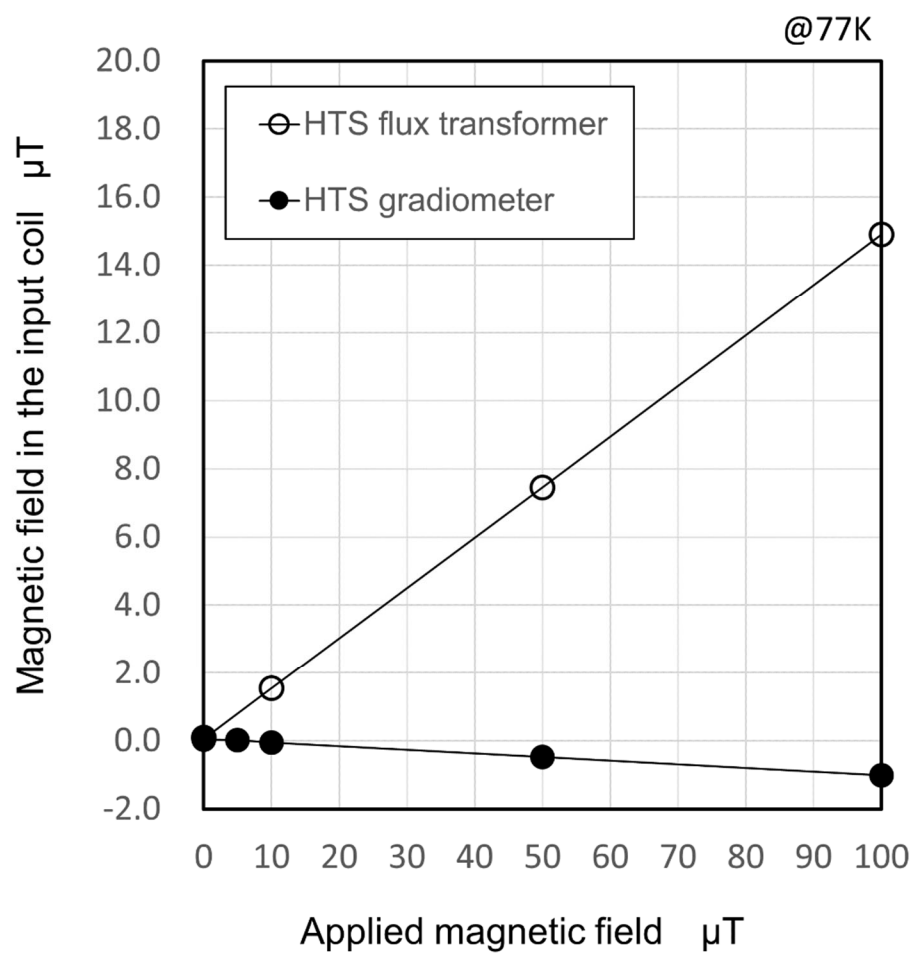


Fig. 6

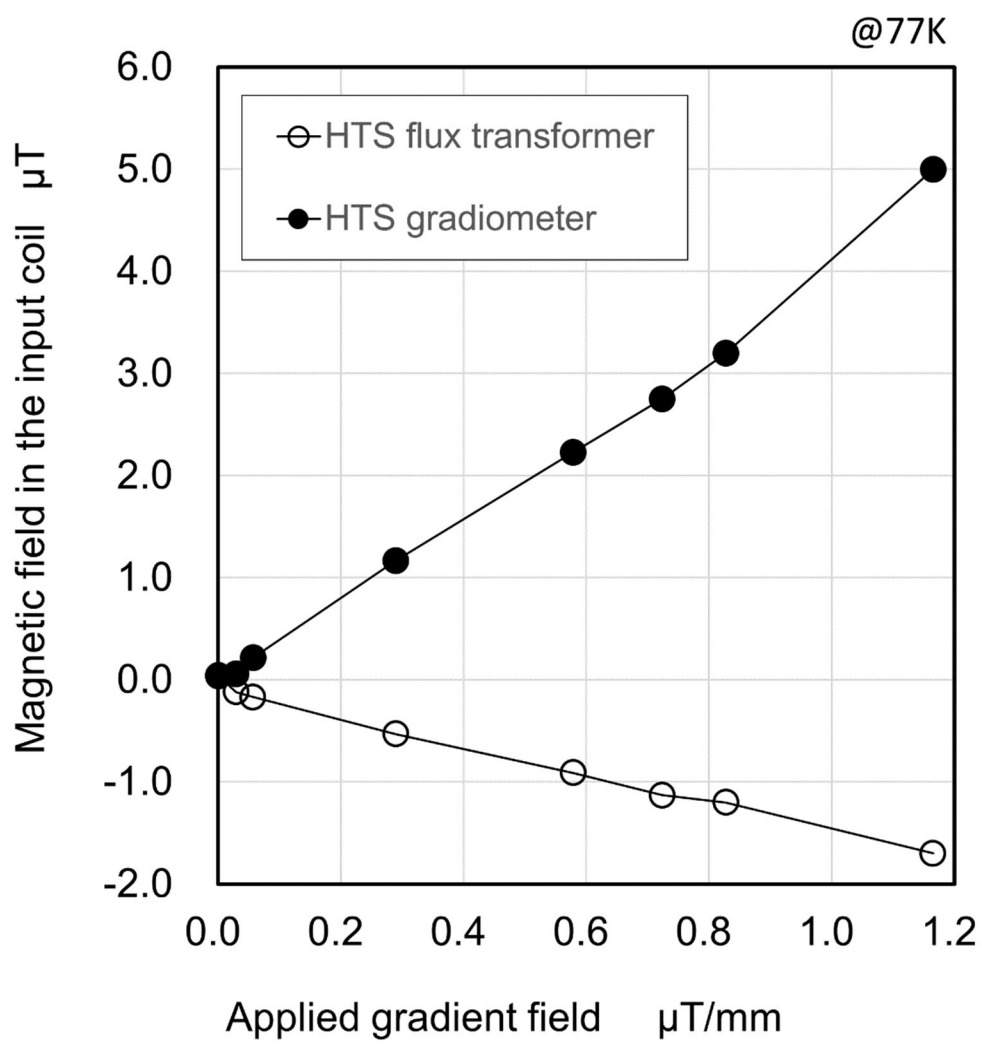


Fig. 7

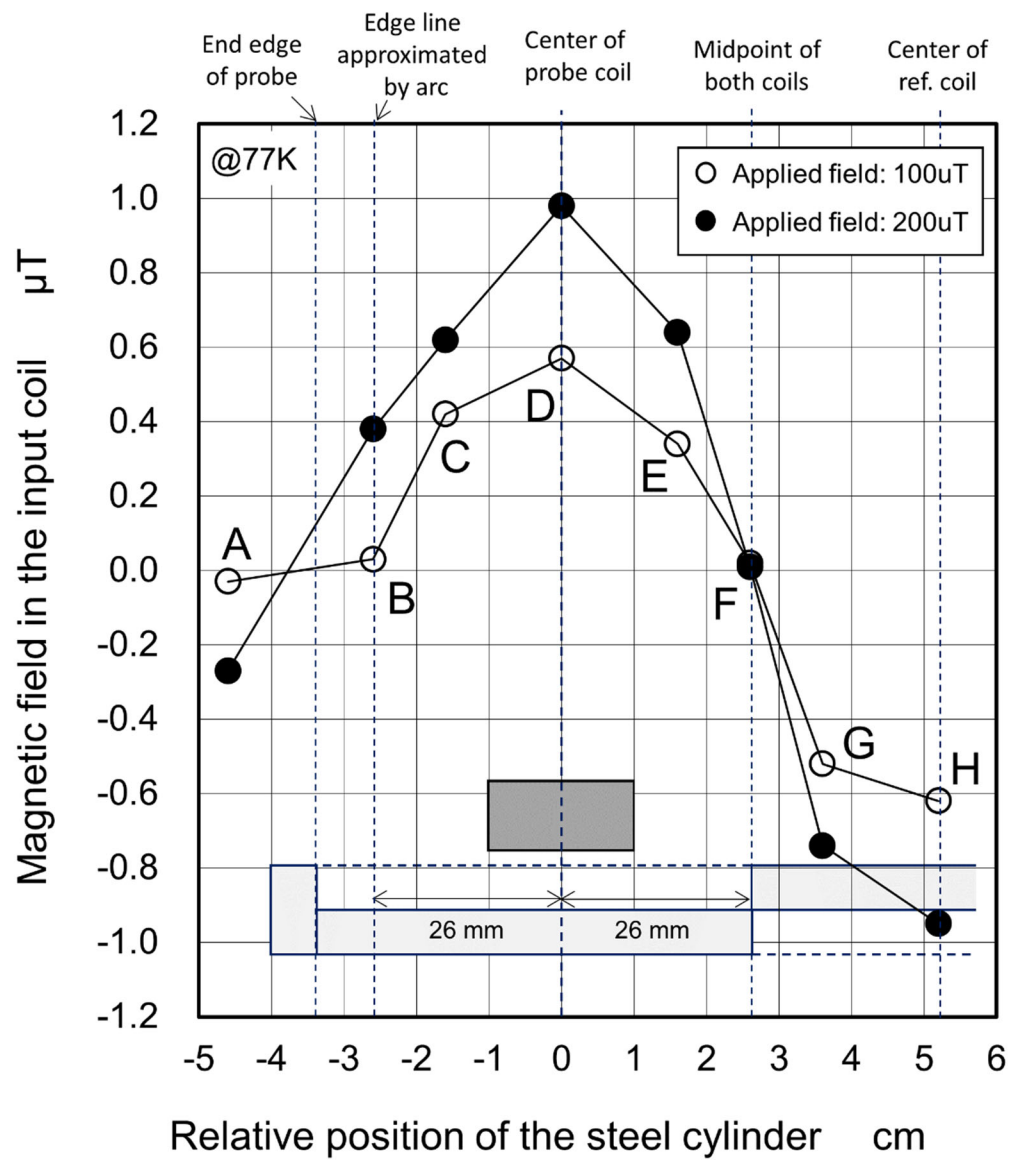


Fig. 8

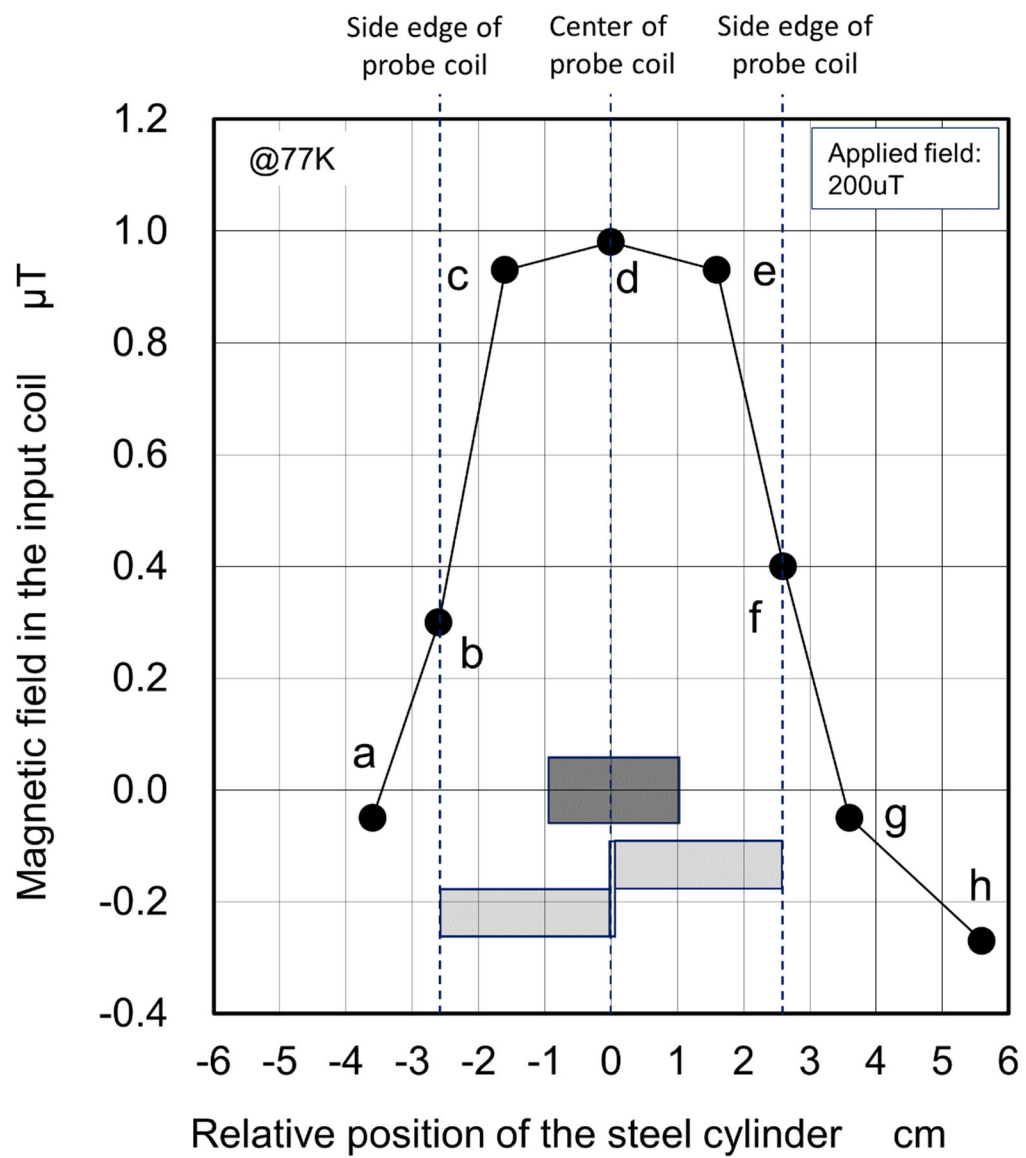


Fig. 9